Electronic Supplementary Material (ESI) for Journal of Materials Chemistry C.

Supporting Information

Effect of annealing conditions on the electrical properties of ALD-grown polycrystalline $BiFeO_3$ films

Iryna S. Golovina[1,2], Matthias Falmbigl[1], Aleksandr V. Plokhikh[1], Thomas C. Parker[3], Craig Johnson[1] and Jonathan E. Spanier[1,4,5*]

[1]*Department of Materials Science & Engineering, Drexel University, Philadelphia, Pennsylvania 19104, USA*

[2]*Institute of Semiconductor Physics, National Academy of Sciences of Ukraine, Kyiv 03028, Ukraine*

[3]*US Army Research Laboratory, Aberdeen Proving Ground, Maryland 21005, USA*

[4]*Department of Electrical & Computer Engineering, Drexel University, Philadelphia, Pennsylvania 19104, USA*

[5]*Department of Physics, Drexel University, Philadelphia, Pennsylvania 19104, USA*

[*]Corresponding Author: spanier@drexel.edu

Structural investigation

Grazing incidence X-ray diffraction (XRD) scans for all samples are displayed in **Figure S1**. In general, longer annealing durations result in higher intensity of the diffraction peaks. The crystal symmetry of the $BiFeO_3$ films cannot be determined from the diffraction patterns. Therefore, pseudocubic (pc) indexation of the BFO was used to determine the lattice parameters. Lattice parameters obtained from the XRD data are presented in Table 1.

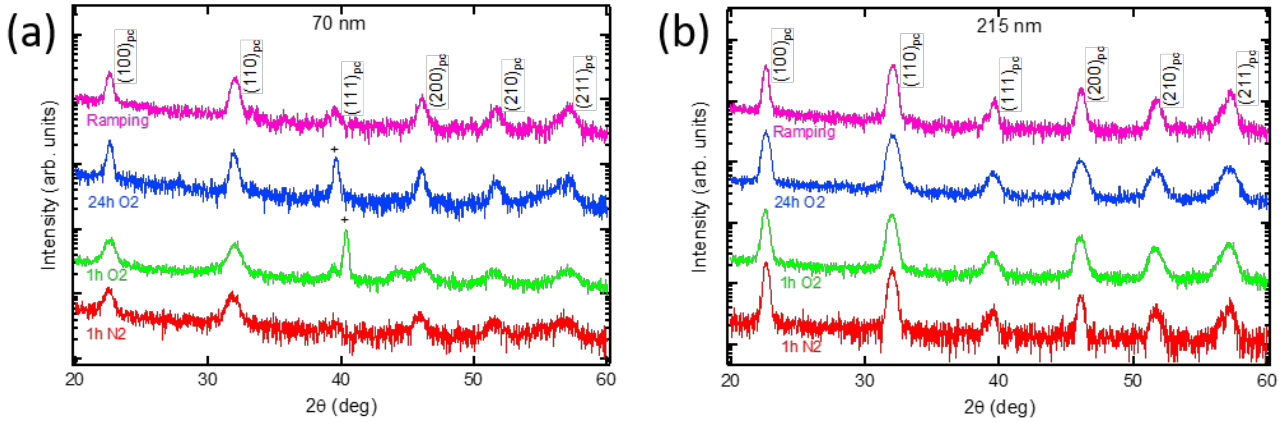

Figure S1. Grazing incidence XRD patterns for the four different annealing conditions for the 70 nm thick films (a) and the 215 nm thick films (b) collected at room temperature. Pseudocubic (pc) indexation of the perovskite phase is provided. '+' denotes peaks corresponding to the substrate. Traces are offset for clarity.

The AFM scans in **Figure S2** show the evolution of the microstructure from the as-grown semi-amorphous to the crystalline state after the annealing step. A snake-like pattern appears after crystallization and becomes enlarged in thinner films (Fig. S2c). Root mean square (RMS) roughness and average grain size values versus annealing procedure and film thickness are summarized in **Table S1**. Note that the roughness increases with longer annealing duration in oxygen atmosphere and with increasing film thickness. The largest grain sizes are obtained after annealing for 24 h in oxygen

atmosphere. As shown in **Table S1**, an average grain size becomes bigger after annealing for 1 h and 24 h in oxygen atmosphere.

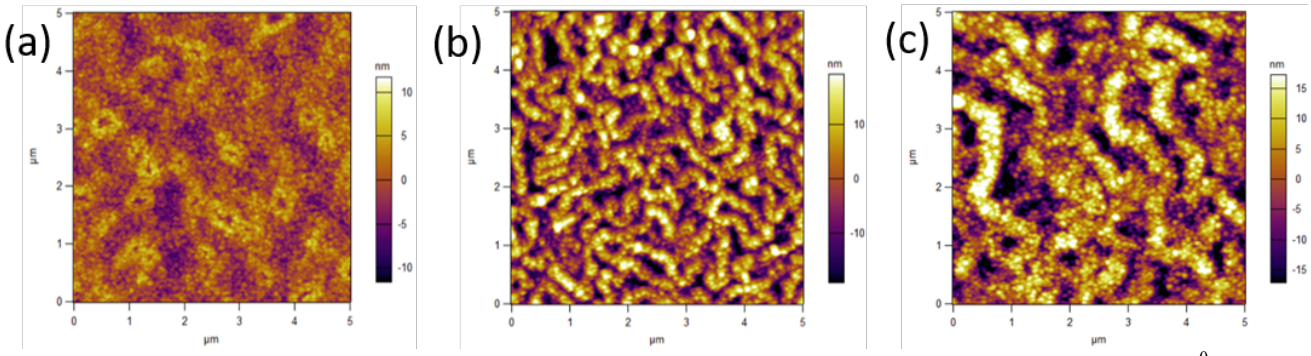

Figure S2. AFM scans of as-deposited (a) film and a 70-nm (b) and a 215-nm (c) thick films each annealed at 550^0C for 1 h in O_2.

Table S1. *RMS and average grain sizes values (in nm) for the 70 nm and 215 nm thick films, annealed at different conditions calculated from an area of 5x5 µm^2.*

Sample	550°C 1h in N_2	550°C 1h in O_2	550°C 24h in O_2	Ramping
70-nm	6.4 / 93	9.0 / 137	7.2 / 226	11.0 / 90
215-nm	10.9 / 95	9.1 / 106	15.3 / 142	18.0 / 98

Compositional analysis

Composition of the films grown on the Pt(111)/Ti/SiO_2/Si(100) substrates after each annealing process was analyzed by energy dispersive spectroscopy (EDS). In order to ensure a reliable measurement of the Bi/Fe-ratio by EDS and to find oxygen content, films on Si substrates were exposed to similar annealing conditions and their composition was determined by Rutherford backscattering spectrometry (RBS). These films with known Bi/Fe-ratio were used as calibration standards for all film compositions measured by EDS. A direct measurement of the composition of BFO films on Pt(111)/Ti/SiO_2/Si(100) substrates by RBS is difficult because of overlapping peak positions.

XPS spectra were collected for four samples, two 70 nm thick films (one annealed for 1 h in O_2 and another under Ramping) and two 215 nm thick samples (one annealed for 1 h in N_2 and another under Ramping). Since Fe^{2+} ions are considered in literature as the source of the leakage current in BFO thin films, we focus here on the iron spectra. The XPS iron spectra and corresponding fits for both 70 nm thick films are displayed in **Figure S3**. All experimental spectra are fitted by six Voigt (Gaussian-Lorentzian) functions: Fe^{3+}2p3/2 at 710.5 eV, Fe^{2+}2p3/2 at 709.4 eV, Fe^{3+}2p1/2 at 724.3 eV, Fe^{2+} 2p1/2 at 723.5 eV, a surface peak at 713.0 eV, and a satellite peak at 718.3 eV. The last two peaks originate from Fe2p3/2 lines, while the shift of binding energy can be explained by charging of the sample surface during XPS measurements and interaction of 2p and 3d shells for surface and satellite peaks, respectively.[1] According to the fitting presented in Fig. S3a, the Fe^{2+}/Fe^{3+} ratio is 0.09 for a 70 nm thick film annealed for 1 h in O_2. It remains unchanged for other annealing regimes. The latter is clearly seen in Fig. S3b, where the raw spectra for two samples are displayed.

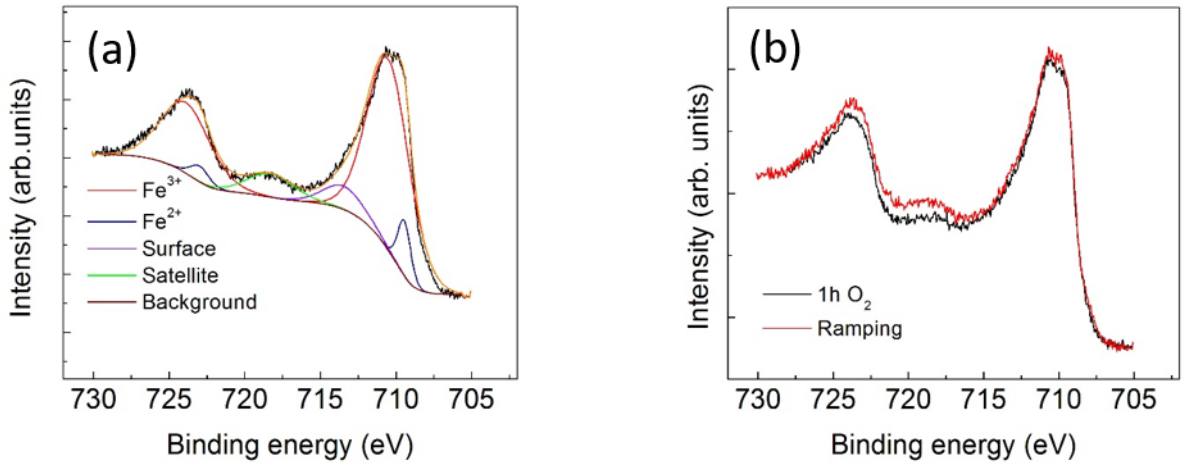

Figure S3. Fitting of the experimental XPS iron spectrum collected for the 70 nm thick film annealed for 1h in O_2 (a) and experimental spectra collected for two 70-nm thick samples, annealed for 1h in O_2 and under Ramping (b).

Ferroelectric behavior

The ability to orient and reorient domains using PFM is shown in **Figure S4**. While the amplitude of the PFM response in the sample annealed in O_2 is comparable with that in epitaxial BFO films, the ability to pole the domains in the polycrystalline film is much lower compared to epitaxial films (*e.g.*, see Fig.4 in Ref. 2). This difference can be attributed to the different orientation of domains in surrounding grains and pinning of domains at the grain boundaries.

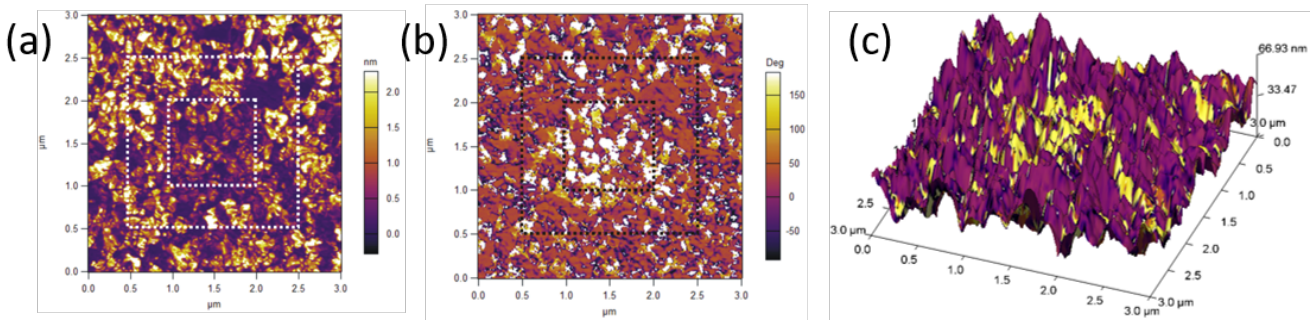

Figure S4. Topographic amplitude (a), phase (b) and overlay of phase on height (c) of the PFM contrast images of the film surface exhibiting patterned domains following writing of two square-shaped regions (one within the other) written using V_{tip} = ± 6 V and using a tip voltage V_{ac} of 200 mV for reading. These data were collected on the 70 nm thick sample annealed for 1 h in O_2.

The macroscopic ferroelectricity of the thin films was probed by collecting polarization-electric field (P-E) hysteresis loops at room temperature. The P-E loops for two representative samples are displayed in **Figure S5**. The magnitude of polarization reflects the difference in leakage current for these samples, which is about one order of magnitude (see Fig.5). While the total polarization obviously caused by leakage current decreases, the remnant polarization increases from 0.12 µC/cm^2 for the sample annealed for 1 h in O_2 to 0.20 µC/cm^2 for the sample annealed for 24 h in O_2. It should be noted that only non-saturated polarization was measured due to the electrical breakdown. Although we obtain a substantial reduction of leakage current after extensive annealing in oxygen, a non-saturated P-E loop can be obtained. Earlier, a non-saturated polarization was registered by S. K. Singh *et al.* for

polycrystalline BFO thin films at room temperature even though the improved leakage current density was as low as 10^{-8} A/cm^2.[3] Recently, a non-saturated P-E dependence with remnant polarization varying from 1 to 5 μC/cm^2 was observed by Puttaswamy *et. al* on 200 nm thick ALD-grown BFO thin films.[4] Furthermore, the ferroelectric properties gradually degrade at thicknesses below 100 nm and the saturation polarization decreases to 3 μC/cm^2 for the 40 nm epitaxial film,[5] while a PFM response is revealed down to 2 nm.[6] Marchand *et al.* demonstrate that a remnant polarization of 20 μC/cm^2 is measured for 500 nm thick polycrystalline BFO film, whereas the values of 0.06 and 0.30 μC/cm^2 are obtained for 50 and 200 nm films, respectively.[7]

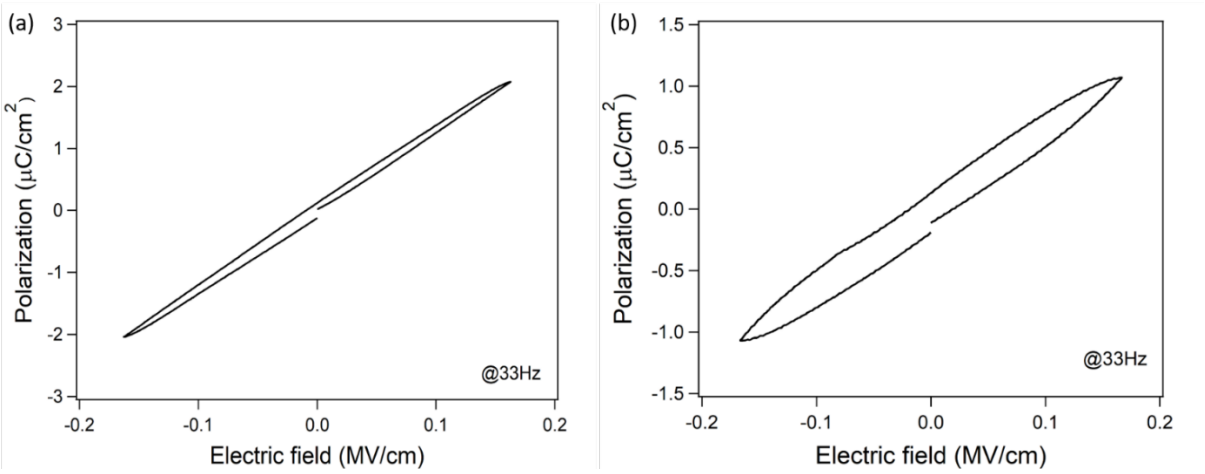

Figure S5. Representative P-E loops for the 215 nm thick film annealed for 1h in O_2 (a) and for 24 h in O_2 (b).

References

1 A. P. Grosvenor, B. A. Kobe, M. C. Biesinger and N. S. McIntyre, *Surf. Interface Anal.*, 2004, **36**, 1564–1574.

2 A. R. Akbashev, G. Chen, J. E. Spanier, *Nano Lett.*, 2013, **14**, 44−49.

3 S. K. Singh and H. Ishiwara, *Japanese Journal of Applied Physics*, 2005, **44**, L734–L736.

4 M. Puttaswamy, M. Vehkamäki, K. Kukli, M. C. Dimri, M. Kemell, T. Hatanpää, M. J. Heikkilä, K. Mizohata, R. Stern, M. Ritala and M. Leskelä, *Thin Solid Films* 2016, **611**, 78–87.

5 Yao Wang, Yuanhua Lin, and Ce-Wen Nan, *J. Appl. Phys*. 2008, **104**, 123912.

6 Y. H. Chu, T. Zhao, M. P. Cruz, Q. Zhan, P. L. Yang, L. W. Martin, M. Huijben, C. H. Yang, F. Zavaliche, H. Zheng, and R. Ramesh, *Appl. Phys. Lett.*, 2007, **90**, 252906.

7 B. Marchand, P. Jalkanen, V. Tuboltsev, M. Vehkamäki, M. Puttaswamy, M. Kemell, K. Mizohata, T. Hatanpa, A. Savin, J. Räisänen, M. Ritala and M. Leskela, *J. Phys. Chem. C,* 2016, **120**, 7313−7322.